ISSN 1392–1207. MECHANIKA. 2022 Volume 28(5): 378–386

Nonlinear State Dependent Sliding Sector Control of Gimbal Systems

Burak Eren BIRINCI*, Bülent ÖZKAN, Metin Uymaz SALAMCI*****
**Defense Industries Research and Development Institute, Ankara, 06261, Turkey, E-mail: burak.birinci@tubitak.gov.tr*
***Gazi University, Faculty of Engineering, Department of Mechanical Engineering, Ankara, 06570 Turkey, E-mail: bozkan@gazi.edu.tr*
****Gazi University, Faculty of Engineering, Department of Mechanical Engineering, Ankara, 06570 Turkey, E-mail: msalamci@gazi.edu.tr*
****Gazi University, Additive Manufacturing Technologies Application and Research Center, Ektam, Ankara, 06570 Turkey, E-mail: msalamci@gazi.edu.tr*

crossref http://dx.doi.org/10.5755/j02.mech.31210

1. Introduction

Sliding Mode Control (SMC) design techniques have been proposed to control linear and nonlinear dynamical systems mainly due to their robustness property to a class of disturbance and parametric uncertainties. In addition to theoretical research studies for the mathematical background of the controller design, some of the research focuses on having a physically applicable controller [1- 4].

One of the drawbacks encountered during the implementation stage of SMC is the chattering phenomenon due to high frequency control signal which occurs when the system trajectories are confined to stay on the sliding surface. In order to eliminate chattering during the sliding mode, various approaches take place in the literature such as imitating the Variable Structure Control (VSC) signal with appropriate smooth functions [1, 5], using adaptive, and variable gain approximations [6, 7], higher-order sliding modes [8, 9] and designing Sliding Sector Control (SSC) [10]. Rather than keeping the trajectories of the system on a hyper-surface in the classical SMC, the system trajectories are bounded inside a sector in the SSC resulting in a relatively smoother control signal. In fact, the hyper-surface of the sliding mode is surrounded by the designed sector in the SSC. Hence the same sliding surface is targeted eventually. The controller of SSC is designed such that the system trajectories are enforced to a predefined stable sector and then left free inside the predefined stable sector. Once the system trajectories are kept inside the stable sector, no further control action is physically needed, and thus, this property is termed as "lazy control" [10]. SSC for linear (continuous and discrete) systems is designed for single-input case in [10] giving the idea of stable linear sectors with some pictorial illustrations. In general, a linear sliding surface is designed and linear sliding sectors are defined for linear time-invariant systems. Afterward, the control is determined so that the system trajectories are steered towards the sector and kept inside it [10].

SSC for nonlinear systems is also suggested with the nonlinear time-varying sliding sector in which State-Dependent Differential Riccati Equation (SDDRE) is solved in order to find the time-varying sliding sector [11]. The method computationally requires the solution of Differential Riccati Equations (DRE) which normally leads one to solve the equations backward since the final conditions are specified only. The authors also suggest a procedure to solve the DRE equations with forward integration algorithm. Moreover, an autopilot is designed for missiles with aerodynamic control surfaces using a sliding sector approach in which a parameter update law is introduced. Disturbances and unmatched uncertainty cases are also considered [12]. The nonlinear sliding sector is used for a MIMO case with the help of multiple sliding sectors and results are demonstrated with an autopilot design of a specific helicopter application [13]. Another application area of sliding sector control is the control of civil structures. Robust time-varying sliding sector control is used for active control of the structure under earthquake vibrations [14]. Although various attempts are presented for the theoretical background of SSC, most of the applications remained limited to simulations. This study proposes a new method for the SSC design and then the proposed method is applied to a gimbal system to implement the algorithm.

Gimbal control in the aviation industry is a highly studied subject due to its usage areas such as missiles and unmanned aerial vehicles. Basics of the gimbal control are given in [15, 16]. Moreover, there are various studies about gimbal and electro-optical systems control with SMC and some of the results are documented. Two-axis gimbal system is controlled and stabilized by using sliding mode control [17], adaptive fractional order sliding mode control [18], integral sliding mode disturbance estimator [19], and adaptive fast terminal sliding mode control with friction compensation [21]. To our best knowledge, this study is the first reported application of nonlinear SSC on axis control of a gimbal system.

In the proposed SSC design procedure, first, a nonlinear (or state-dependent) sliding surface is designed using SDDRE. The State Dependent Riccati Equation (SDRE) method provides a systematic solution to the controller design for a class of nonlinear systems by freezing the nonlinear system at some certain time intervals and considering the frozen system as Linear Time-Invariant (LTI) [22, 23]. The resulting controller has state-dependent feedback gains and/or surface parameters, which allow the controller to cope with the nonlinearities. Therefore, similar to the controller design, the sliding surface in SMC could also be formed by using [24]. The sliding sector around the surface is then designed using the SDDRE and therefore a "state-dependent" (or nonlinear) sliding sector is created. SSC is designed to force the trajectories of the nonlinear system inside the sector. In this study, by introducing new results, the SSC is designed such that the variations of sliding surface and sector are included in the control term unlike the method suggested earlier in [25, 26]. The proposed method in this study is developed for

nonlinear systems under the disturbance for tracking requirements. To cope with the tracking command, the integral of the error signal is supplemented as an augmented state. The controller gains are selected according to the disturbance consideration. Unlike the previously reported results 26, instead of the lazy control approach with hysteresis function, a control signal depending on the sector boundaries is derived within the sector in the proposed method. The methodology is experimentally validated with the inner axis of a two axes gimbal system, where the outer axis oscillates.

The paper is organized as follows: in the next section, mathematical preliminaries and SSC for nonlinear systems are given. The main results are also given in the next section. The suggested SSC design methodology is illustrated on a gimbal system as presented in section 3 and experimental results are presented in section 4. Finally, conclusions are discussed for future extensions of the proposed method in section 5.

2. State dependent sliding sector control

In this section, a new approach to the SSC design for a class of single input nonlinear systems is introduced.

Consider the following single input nonlinear system, where the pair $\left(A(x),b(x)\right)$ is assumed to be a pointwise controllable pair for all $x \in R^n$.

$$\dot{x} = A(x)x(t) + b(x)\left(u(t) + d(x,t)\right), \tag{1}$$

where: $A(x) \in R^{n\times n}$ and $b(x) \in R^{n\times 1}$ are state-dependent system matrices; $u(t) \in R^1$ is the control input and the uncertainty $d(x,t)$ is a bounded scalar function which is defined by:

$$|d(x,t)| \le \gamma(x,t)\|x\| + \beta(t), t \in R^+, x \in R^n, \tag{2}$$

where: $\gamma(x,t)$ and $\beta(t)$ are known positive functions and $\|x\|$ is the norm of x vector.

For the tracking control purpose, define now the following augmented state:

$$e(t) = \int \left(r(t) - Cx(t)\right)dt. \tag{3}$$

Therefore, the derivative of the augmented state is

$$\dot{e}(t) = r(t) - Cx(t). \tag{4}$$

Then the new system equations, including the augmented state become:

$$\dot{\hat{x}} = \hat{A}(\hat{x})\hat{x}(t) + \hat{b}(\hat{x})\left(u(t) + d(\hat{x},t)\right) + Dr(t), \tag{5}$$

where,

$$\hat{x} = \begin{bmatrix} e(t) \\ x(t) \end{bmatrix}, \hat{A}(\hat{x}) = \begin{bmatrix} 0 & -C \\ 0 & A(x) \end{bmatrix}, \tag{6}$$

$$\hat{b}(\hat{x}) = \begin{bmatrix} 0 \\ b(x) \end{bmatrix}, D = \begin{bmatrix} 1 \\ 0 \end{bmatrix}. \tag{7}$$

2.1. Sliding sector design

SSC design approach for the LTI case is proposed in [10] and then extended to nonlinear systems in [25] and in [26] by using the notion of state dependent sliding sectors. In this paper, the same definitions are used for the sliding surface and sector design as in [25] and [26] for the sake of completeness. The sliding surface, $s(\hat{x},t)$, the slope matrix of the sliding surface $S(\hat{x},t)$, sliding sector domain *S*, and the sliding sector $\delta(\hat{x})$, are given as follows:

$$S = \left\{\hat{x} \mid s^2(\hat{x},t) \le \delta^2(\hat{x}), \hat{x} \in R^{n+1}, t \in R^+\right\}, \tag{8}$$

$$s(\hat{x},t) = S(\hat{x},t)\hat{x}(t), S(\hat{x},t) \in R^{1\times n+1}, \tag{9}$$

$$\delta(\hat{x}) = \sqrt{\hat{x}^T(t)\Delta(\hat{x})\hat{x}(t)},\ \Delta(\hat{x}) \in R^{(n+1)\times(n+1)} \ge 0, \tag{10}$$

$$S(\hat{x},t) = \hat{b}^T(\hat{x})P(\hat{x},t), \Delta(\hat{x}) = Q(\hat{x}) - R(\hat{x}), \tag{11}$$

$$R(\hat{x}) = (1-r)Q(\hat{x}), 0 < r < 1, \tag{12}$$

where: $P(\hat{x},t)$ is the state-dependent positive definite symmetric matrix determined from the following SDDRE:

$$\dot{P}(\hat{x},t) + P(\hat{x},t)A(\hat{x}) + A^T(\hat{x})P(\hat{x},t) - P(\hat{x},t)\hat{b}(\hat{x})\hat{b}^T(\hat{x})P(\hat{x},t) + Q(\hat{x}) = 0, \tag{13}$$

where: $Q(\hat{x}) \in R^{(n+1)\times(n+1)}$ positive definite design matrix. Differential Riccati Equation (DRE) is solved for a given positive definite $Q(\hat{x})$ by using a frozen system at each sampling instant according to the current states (See [27] and the references therein for recent computational approaches of SDRE and SDDRE control). Since the solution matrix of DRE; $P(\hat{x},t)$ is state-dependent and the resulting sliding surface is actually time-varying, the designed sliding sector using $P(\hat{x},t)$ is also state-dependent and time-varying.

For the state-dependent nonlinear sliding sector defined in Eq. (8) the following Lyapunov function could be defined as:

$$L = \left(\hat{x}^T(t)P(\hat{x},t)\hat{x}(t)\right) > 0, \forall \hat{x} \in R^{n+1}, (\hat{x} \ne 0), \forall t \in R^+, \tag{14}$$

which decreases with an appropriate SSC law so that the derivative of Lyapunov function along the trajectory of the nonlinear system given by Eq. (5) satisfies the inequality given below:

$$\dot{L} = \frac{d}{dt}\left(\hat{x}^T(t)P(\hat{x},t)\hat{x}(t)\right) \le 0, \forall \hat{x} \in S. \quad (15)$$

2.2. Controller design

Having designed the sliding sector, one can determine the SSC law by using the following theorem, which is the main result of this paper.

Lemma 1 (Barbalat's Lemma). If the differentiable function $L(t)$ has a finite limit as $t \to \infty$ and if it is uniformly continuous, then $\dot{L}(t) \to 0$ as $t \to \infty$ [28]

Proof. See [28]

Theorem 2. Consider the single input nonlinear system given by Eq. (5). Suppose that the nonlinear sliding sector as defined by Eq. (8) is determined by solving the SDDRE given by Eq. (13). Then the following sliding sector control law forces the system trajectories towards the sliding sector inside which the system stability is ensured.

$$u(t) = \begin{cases} u_i(t), s^2(\hat{x},t) \le \delta^2(\hat{x}) \\ u_o(t), s^2(\hat{x},t) > \delta^2(\hat{x}) \end{cases} \quad (16)$$

$$u_o(t) = -\left(S(\hat{x},t)\hat{b}(\hat{x})\right)^{-1}\left(S(\hat{x},t)\hat{A}(\hat{x})\hat{x}(t) + K_1(\hat{x})s(\hat{x},t) + \dot{S}(\hat{x},t)\hat{x}(t) + S(\hat{x},t)Dr(t)\right), \quad (17)$$

$$u_i(t) =$$

$$= -\left(S(\hat{x},t)\hat{b}(\hat{x})\right)^{-1}\left(S(\hat{x},t)\hat{A}(\hat{x})\hat{x}(t) + K_1(\hat{x})s(\hat{x},t) + K_2(\hat{x})\rho(x,t)\hat{x}(t) + S(\hat{x},t)Dr(t) + k(\hat{x})\delta(\hat{x})sign\left(s(\hat{x},t)\right)\right), \quad (18)$$

where,

$$\rho(x,t) = \frac{\dot{S}(\hat{x},t)\dot{S}^T(\hat{x},t)}{S(\hat{x},t)S^T(\hat{x},t)}, \quad (19)$$

and $K_1(\hat{x})$, $K_2(\hat{x})$ and $k(\hat{x})$ satisfy the following inequalities, respectively.

$$K_1(\hat{x}) > max\left\{\left\|\frac{\left(S(\hat{x},t)\hat{b}(\hat{x})\right)}{2}\right\|, \left\|\frac{S(\hat{x},t)\hat{b}(\hat{x})\left(\gamma(\hat{x})\|x\| + \beta(t)\right)}{s(\hat{x},t)}\right\|\right\}, \quad (20)$$

where: $s(\hat{x},t) \neq 0; \forall \|\hat{x}\| \neq 0$.

$$S^T(\hat{x},t)S(\hat{x},t)A(\hat{x}) + S^T(\hat{x},t)K_2(\hat{x})\rho(\hat{x},t)S(\hat{x},t) \ge 0, \quad (21)$$

$$k(\hat{x}) > \left\|\frac{S(\hat{x},t)b(\hat{x})d(\hat{x},t)}{\delta(\hat{x},t)}\right\|; \quad \delta(\hat{x},t) \neq 0; \forall \|\hat{x}\| \neq 0. \quad (22)$$

Proof. *Case 1.* When the states of the nonlinear system stay outside the sector, i.e. $|s(\hat{x},t)| > \delta(\hat{x})$, the trajectories should be directed to the sliding surface. Therefore, by considering the sliding surface function defined in Eq. (8), the derivative will be,

$$\dot{s}(\hat{x},t) = S(\hat{x},t)\dot{\hat{x}}(t) + \dot{S}(\hat{x},t)\hat{x}(t)$$

For the outside of the sector, by using the control term defined in Eq. (17) the expression becomes:

$$\frac{d}{dt}s^2(\hat{x},t) = 2s(\hat{x},t)\dot{s}(\hat{x},t) = 2s(\hat{x},t)\left[S(\hat{x},t)\dot{\hat{x}}(t) + \dot{S}(\hat{x},t)\hat{x}(t)\right] =$$

$$= 2s(\hat{x},t)\begin{bmatrix} S(\hat{x},t)\left(\hat{A}(\hat{x})\hat{x}(t) + \hat{b}(\hat{x})\left(u(t) + d(\hat{x},t)\right) + Dr(t)\right) \\ +\dot{S}(\hat{x},t)\hat{x}(t) \end{bmatrix},$$

$$\frac{d}{dt}s^2(\hat{x},t) = 2s(\hat{x},t)\begin{bmatrix} S(\hat{x},t)\hat{A}(\hat{x})\hat{x}(t) + \dot{S}(\hat{x},t)\hat{x}(t) \\ +S(\hat{x},t)\hat{b}(\hat{x})\left(-\left(S(\hat{x},t)\hat{b}(\hat{x})\right)^{-1}\left(S(\hat{x},t)\hat{A}(\hat{x})\hat{x}(t) + K_1(\hat{x})s(\hat{x},t) + \dot{S}(\hat{x},t)\hat{x}(t) + S(\hat{x},t)Dr(t)\right)\right) \\ +S(\hat{x},t)\hat{b}(\hat{x})d(\hat{x},t) + S(\hat{x},t)Dr(t) \end{bmatrix} =$$

$$= 2s(\hat{x},t)\left[-K_1(\hat{x})s(\hat{x},t) + S(\hat{x},t)\hat{b}(\hat{x})d(\hat{x},t)\right] = -2K_1(\hat{x})s^2(\hat{x},t) + 2s(\hat{x},t)S(\hat{x},t)\hat{b}(\hat{x})d(\hat{x},t).$$

By choosing $K_1(\hat{x})$ as follows:

$$K_1(\hat{x}) > \left\|\frac{\left(S(\hat{x})\hat{b}(\hat{x})\right)\left(\gamma(x,t)\|x\| + \beta(t)\right)}{s(\hat{x},t)}\right\|,$$

where: $s(\hat{x},t) \neq 0; \forall \|\hat{x}\| \neq 0$.

The reachability condition, $s(\hat{x},t)\dot{s}(\hat{x},t) < 0$, is satisfied which implies that the absolute value of $s(\hat{x},t)$ will decrease so that the states of system given by Eq. (5)

moves towards inside the sector.

Case 2. While the system state moves towards inside the sector with the control law given by Eq. (18), the so-called P-norm of a system decreases. Consider now the Lyapunov function candidate as defined by:

$$L(t)=\hat{x}^T(t)P(\hat{x},t)\hat{x}(t)>0,\forall\hat{x}\in R^{n+1},$$
$$(\hat{x}\neq 0),\forall\in R^{+}, \tag{23}$$

Then the time derivative of Lyapunov function along the trajectories is;

$$\dot{L}(t)=\dot{\hat{x}}^T(t)P(\hat{x},t)\hat{x}(t)+\hat{x}^T(t)\dot{P}(\hat{x},t)\hat{x}(t)+\hat{x}^T(t)P(\hat{x},t)\dot{\hat{x}}(t)=$$
$$=\left(\hat{x}^T(t)\hat{A}^T(\hat{x})+u(t)\hat{b}^T(\hat{x})+d^T(\hat{x},t)\hat{b}^T(\hat{x},t)+r^T(t)D^T\right)P(\hat{x},t)\hat{x}(t)+\hat{x}^T(t)\dot{P}(\hat{x},t)\hat{x}(t)+$$
$$+\hat{x}^TP(\hat{x},t)\begin{pmatrix}\hat{A}(\hat{x})\hat{x}(t)+\hat{b}(\hat{x})u(t)\\+\hat{b}(\hat{x})d(\hat{x},t)+Dr(t)\end{pmatrix}=\hat{x}^T(t)\left(\hat{A}^T(\hat{x})P(\hat{x},t)+P(\hat{x},t)\hat{A}(\hat{x})+\dot{P}(\hat{x},t)\right)\hat{x}(t)+$$
$$+2\hat{x}^T(t)P(\hat{x},t)\hat{b}(\hat{x})u(t)+2\hat{x}^T(t)P(\hat{x},t)\hat{b}(\hat{x})d(\hat{x},t)+2\hat{x}^T(t)P(\hat{x},t)Dr(t)=$$
$$=-\hat{x}^T(t)Q(\hat{x})\hat{x}(t)+\hat{x}^T(t)P(\hat{x},t)\hat{b}(\hat{x})\hat{b}^TP(\hat{x},t)\hat{x}(t)+2\hat{x}^T(t)P(\hat{x},t)\hat{b}(\hat{x})d(\hat{x},t)+$$
$$+2\hat{x}^T(t)P(\hat{x},t)Dr(t)+2\hat{x}^T(t)P(\hat{x},t)\hat{b}(\hat{x})$$
$$\left[-\left(S(\hat{x},t)\hat{b}(\hat{x})\right)^{-1}\left(S(\hat{x},t)\hat{A}(\hat{x})\hat{x}(t)+K_1(\hat{x})s(\hat{x},t)+K_2(\hat{x})\rho(\hat{x},t)\hat{x}(t)+S(\hat{x},t)Dr(t)+k(\hat{x})\delta(\hat{x})sign(s(\hat{x},t))\right)\right].$$

Note that, $b^T(\hat{x})P(\hat{x},t)=P(\hat{x},t)b(\hat{x})=s(x,t)$. So the derivative of the Lyapunov function is re-defined in two parts as in the following fashion.

$$\dot{L}(t)=W_1+W_2, \tag{24}$$

$$W_1=-\left[2\left(S(\hat{x},t)\hat{b}(\hat{x})\right)^{-1}K_1(\hat{x})-1\right]s^2(\hat{x},t)-2\left(S(\hat{x},t)\hat{b}(\hat{x})\right)^{-1}\hat{x}^T(t)\begin{pmatrix}S^T(\hat{x},t)S(\hat{x},t)A(\hat{x})\\+S^T(\hat{x},t)\rho(\hat{x},t)S(\hat{x},t)\end{pmatrix}\hat{x}(t)-$$
$$-2\left(S(\hat{x},t)\hat{b}(\hat{x})\right)^{-1}\left(k(\hat{x})\delta(\hat{x})|s(\hat{x},t)|+2s(\hat{x},t)d(\hat{x},t)\right), \tag{25}$$

$$W_2=-\hat{x}^T(t)Q(\hat{x})\hat{x}(t)+2\hat{x}^T(t)P(\hat{x},t)g(\hat{x}). \tag{26}$$

By choosing the gains as given in Eqs. (20), (21) and (22), the first term of the derivative of the Lyapunov function W_1 will be negative semi-definite.

Similarly, the second term of the derivative of the Lyapunov function W_2 is defined as follows.

$$W_2=-\hat{x}^T(t)Q(\hat{x})\hat{x}(t)+2\hat{x}^T(t)P(\hat{x},t)g(\hat{x})\leq$$
$$\leq-\lambda_{min}\left(Q(\hat{x})\right)\|\hat{x}\|+2\lambda_{max}\left(P(\hat{x},t)\right)\|\hat{x}\|\|g(\hat{x})\|\leq$$
$$\leq-\|(\hat{x})\|\lambda_{max}\left(P(\hat{x},t)\right)\left(\epsilon\|\hat{x}\|-2\|g(\hat{x})\|\right).$$

where: $\epsilon=\dfrac{\lambda_{min}\left(Q(\hat{x},t)\right)}{\lambda_{max}\left(P(\hat{x},t)\right)}$ so that $g(\hat{x})$ satisfies the equation given below.

$$\|g(\hat{x})\|\leq\frac{1}{2}\epsilon\|\hat{x}\|. \tag{27}$$

W_2 is negative semi-definite with the condition that is given in Eq. (27). Considering the Eq. (24) with the results of W_1 and W_2, the derivative of the Lyapunov function Eq. (15) becomes negative semi-definite with Eq. (18) and Lemma 1, thus the system stability is ensured which completes the proof of the theorem.

Notice that, the proposed SSC algorithm given by Eq. (16) uses the solution of SDDRE defined in Eq. (13). Since the sliding surface together with the sliding sectors varies with states, they alter in time as well. Therefore, the derivatives of the sliding surface parameters are also included in the SSC. By this way, sign of the Lyapunov function term related to the gain $K_2(\hat{x},t)$ given by Eq. (21) becomes negative.

2.3. A simulation study

The control approach defined in Theorem 2 is applied to a fictitious system. The following nonlinear second-order system 29 is considered.

$$\dot{x}_1=x_2,$$

$$\dot{x}_2=2x_1\sin x_2+3|x_2|\cos x_1+u.$$

To convert the regulator problem to a tracking one, an augmented state is included. In this case, the state space representation of the fictitious system is given as follows:

$$\begin{bmatrix}\dot{e}\\\dot{x}_1\\\dot{x}_2\end{bmatrix}=\begin{bmatrix}0&-1&0\\0&0&1\\0&2\sin x_2&3|x_2|(x_2)^{-1}\cos x_1\end{bmatrix}\begin{bmatrix}e\\x_1\\x_2\end{bmatrix}+\begin{bmatrix}0\\0\\1\end{bmatrix}u+\begin{bmatrix}1\\0\\0\end{bmatrix}r.$$

The weighting matrix is selected as $Q = diag\left\{9.9\times10^{7},1,1\right\}$. In the simulation, reference input is set as a step command and sinusoidal command respectively. Fig. 1 shows the time response of the states of the system. Also, the control input of the system is given in Fig. 2. Changes of sliding surface and sliding sector over time are given in Fig. 3. The evolution of the controller gains is given in Fig. 4. In this example, the controller gains K_1, K_2 and k are varied as state dependently according to the equations (20) through (22) respectively.

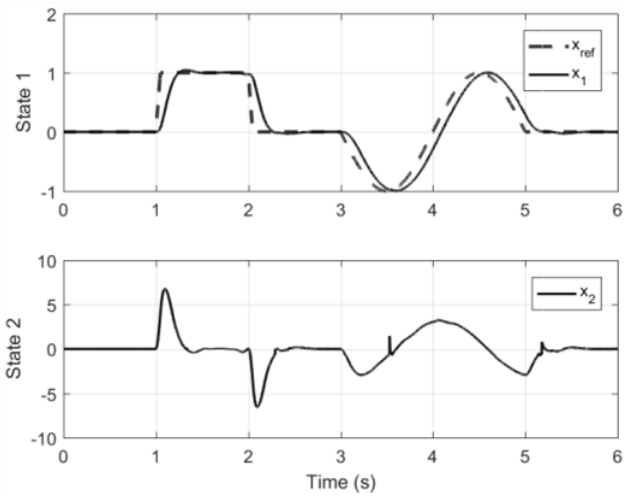

Fig. 1 State-1 and State-2 of the fictitious system

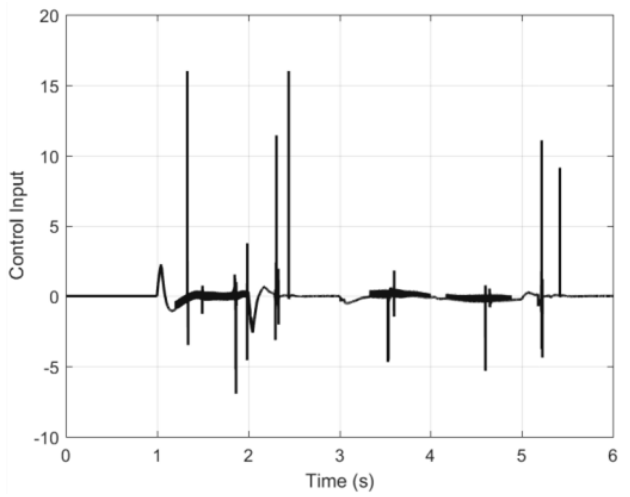

Fig. 2 Control input of the fictitious system

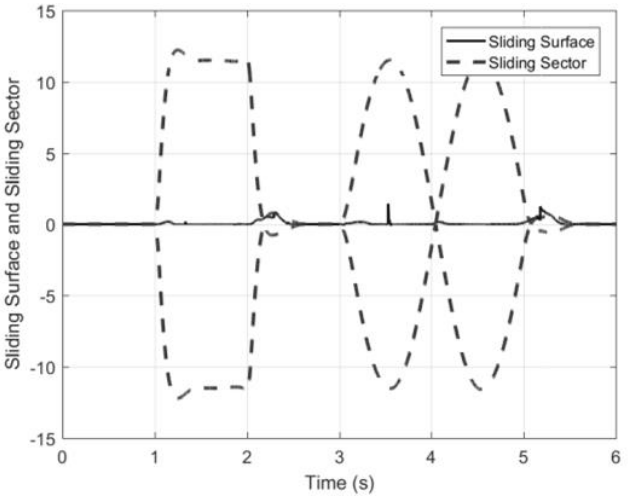

Fig. 3 Evolution of the sliding surface and sliding sectors of the fictitious system

3. Gimbal system

The method proposed in this paper is applied to an inner axis of a two axes pitch-yaw gimbal system as shown in Fig. 5.

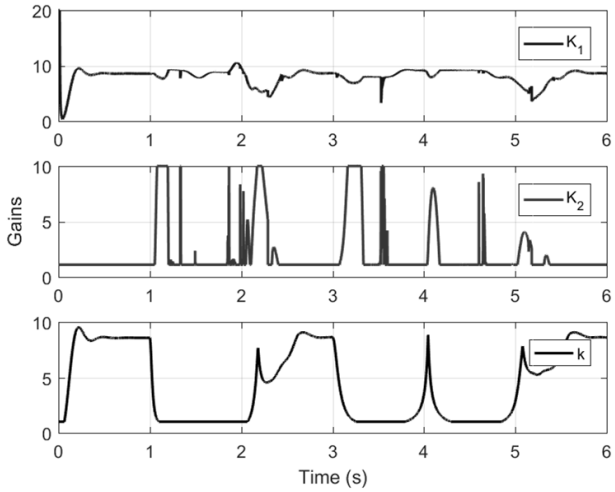

Fig. 4 Evolution of the controller gains of the fictitious system

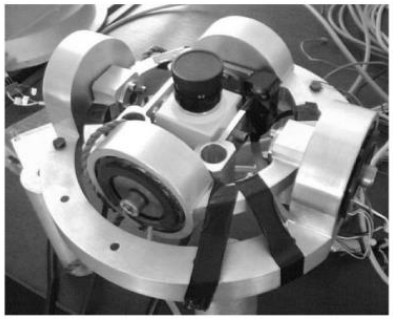

Fig. 5 Two axes pitch yaw gimbal system

The equations of the motion of the gimbal can be derived by applying the Lagrange equation given below.

$$\frac{d}{dt}\left(\frac{\partial K}{\partial \dot{q}_j}\right)-\frac{\partial K}{\partial q_j}+\frac{\partial U}{\partial q_j}+\frac{\partial D}{\partial \dot{q}_j}=\Theta_j, \tag{28}$$

where the kinetic energy function is:

$$K=\frac{1}{2}\omega_o^T J_o\omega_o+\frac{1}{2}\omega_i^T J_i\omega_i=$$

$$=\frac{1}{2}\begin{bmatrix}0 & \dot{\theta} & 0\end{bmatrix}\begin{bmatrix}J_{ox} & 0 & 0\\ 0 & J_{oy} & 0\\ 0 & 0 & J_{oz}\end{bmatrix}\begin{bmatrix}0\\ \dot{\theta}\\ 0\end{bmatrix}+$$

$$+\frac{1}{2}\begin{bmatrix}\dot{\theta}\sin\psi & \dot{\theta}\cos\psi & \dot{\psi}\end{bmatrix}\begin{bmatrix}J_{ix} & 0 & 0\\ 0 & J_{iy} & 0\\ 0 & 0 & J_{iz}\end{bmatrix}\begin{bmatrix}\dot{\theta}\sin\psi\\ \dot{\theta}\cos\psi\\ \dot{\psi}\end{bmatrix}.$$

$$K=\frac{1}{2}\left[\dot{\theta}^2\left(J_{oy}+J_{iy}\sin^2\psi+J_{iy}\cos^2\psi\right)+\dot{\psi}^2 J_{iz}\right]. \tag{29}$$

Similarly, the potential energy function is:

$$U = \frac{1}{2}\left[K_o\theta^2 + K_i\psi^2\right]. \quad (30)$$

Dissipative energy due to frictions is:

$$D = \frac{1}{2}\omega_o^T B_o \omega_o + \frac{1}{2}\omega_i^T B_i \omega_i. \quad (31)$$

The parameters of the gimbal and its descriptions are given in Table 1

Table 1

Description of the Gimbal's Parameters

Symbol	Description
o	indices for outer axis parameters
i	indices for inner axis parameters
1, 2, 3	indices for axis x, y, z respectively
$\psi,\dot{\psi}$	yaw angle and yaw rate
$\theta,\dot{\theta}$	pitch angle and pitch rate
K_j	spring constant of axis $\left(j = i \ and \ o\right)$
B_j	viscous friction of axis $\left(j = i \ and \ o\right)$
J_{jk}	moments of inertia matrix of axis $\left(j = i \ and \ o\right)\left(k = 1,2 \ and \ 3\right)$
T_j	motor torque $\left(j = i \ and \ o\right)$
i_j	motor current $\left(j = i \ and \ o\right)$
K_t	torque constant of the BLDC motor

3.1. Equations of motion of the yaw axis of the gimbal system

Yaw axis constitutes to the inner axis of the gimbal system and its equation of motion is given below.

$$\frac{d}{dt}\left(\frac{\partial K}{\partial \dot{\psi}}\right) = \ddot{\psi} J_{iz}, \ \frac{\partial K}{\partial \psi} = \dot{\theta}^2 \sin\psi\cos\psi\left(J_{ix} - J_{iy}\right),$$

$$\frac{\partial U}{\partial \psi} = K_i\psi, \ \frac{\partial D}{\partial \dot{\psi}} = \dot{\psi} B_i, \ T_i = K_t i_i.$$

$$\ddot{\psi} J_{iz} + \dot{\psi} B_i + \psi K_i - \dot{\theta}^2 \sin\psi\cos\psi\left(J_{ix} - J_{iy}\right) = K_t i_i. \quad (32)$$

State-space representation of the yaw axis dynamics for position control is now as follows:

$$x_1 = \psi, \quad (33)$$

$$x_2 = \dot{\psi}, \quad (34)$$

$$\begin{bmatrix}\dot{x}_1\\ \dot{x}_2\end{bmatrix} = \begin{bmatrix}0 & 1\\ -\frac{K_i}{J_{iz}} + \frac{F(x)}{J_{iz}\left(x_1 + \epsilon\right)} & -\frac{B_i}{J_{iz}}\end{bmatrix}\begin{bmatrix}x_1\\ x_2\end{bmatrix} + \begin{bmatrix}0\\ \frac{K_t}{J_{iz}}\end{bmatrix} i_i, \quad (35)$$

$$y_i = \begin{bmatrix}1 & 0\end{bmatrix}\begin{bmatrix}x_1\\ x_2\end{bmatrix}, \quad (36)$$

where: $F(x) = \dot{\theta}^2 \sin(x_1)\cos(x_1)\left(J_{ix} - J_{iy}\right)$ and ϵ is a sufficiently small number added to avoid uncertainty. The integral action approach could be used to convert the regulator problem to a tracking one. In this case, the expression of the system in the state space appears in the following manner:

$$e = \int\left(r_i - y_i\right)dt. \quad (37)$$

$$\begin{bmatrix}\dot{e}\\ \dot{x}_1\\ \dot{x}_2\end{bmatrix} = \begin{bmatrix}0 & -1 & 0\\ 0 & 0 & 1\\ 0 & -\frac{K_i}{J_{iz}} + \frac{F(x)}{J_{iz}\left(x_1 + \epsilon\right)} & -\frac{B_i}{J_{iz}}\end{bmatrix}\begin{bmatrix}e\\ x_1\\ x_2\end{bmatrix} + \begin{bmatrix}0\\ 0\\ \frac{K_t}{J_{iz}}\end{bmatrix} i_i + \begin{bmatrix}1\\ 0\\ 0\end{bmatrix}\psi_{ref}.$$

where: ϵ is a small number that was added to the system equations to prevent singularity in the case of x_1 is equal to zero. The parameters of the yaw axis are given in Table 2.

Table 2

Parameters of the yaw axis

Symbol	Value	Unit
K_i	0.095	N.m/rad
B_i	0.02	N.m.s/rad
J_{ix}	696.5×10^{-6}	kg.m^2
J_{iy}	898.6×10^{-6}	kg.m^2
J_{iz}	472.8×10^{-6}	kg.m^2
K_i	0.0328	N.m/A.

4. Experimental results

The parameters of the sliding sector and controller, which are used in the experiments, are given in Table 3

Table 3

Parameters of the sliding sector control

Symbol	Value
Q	$\begin{bmatrix}98\times10^7 & 0 & 0\\ 0 & 1 & 0\\ 0 & 0 & 1\end{bmatrix}$
R	$0.1\times Q$
K_1	$4.8\times e^{\left(\psi_{ref} - \psi\right)}$
K_2	$18\times e^{\psi}$
k	0.05

The SSC law developed in section 2, is applied to the two axes gimbal system. The results of the experiments are given in this section. During the experiments, the outer axis of the gimbal system is excited by input of 5^o amplitude and 0.5 Hz frequency simultaneously with the inner axis regarding the proposed SSC. Runge Kutta method is used in each time interval for the real-time solution of the SDDRE. The experimental setup contains motor drivers to control the electromechanical system, input-output cards to

collect data from resolvers, and terminal blocks for cable pin connections. The real-time application is run on the target computer at a 2 kHz sampling frequency. Throughout the test, step and sinusoidal position commands are applied, respectively. Before the step command, 0.25 Nm disturbance effect is applied on the axis to test the robustness of the system with the proposed controller. The experimental results are given in Fig. 6 through Fig. 9.

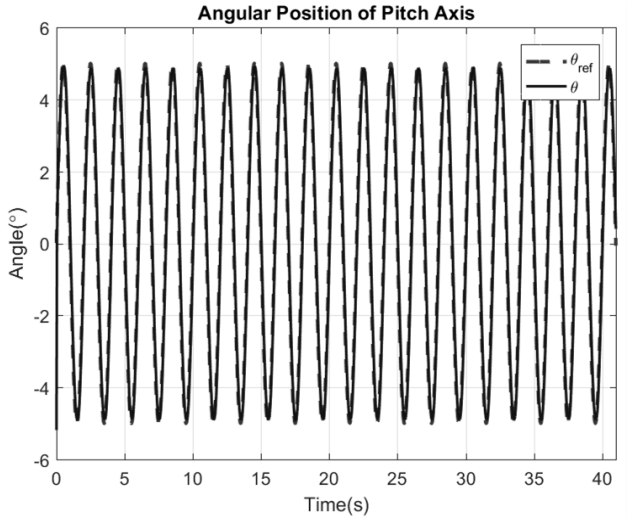

Fig. 6 Angular position of the pitch axis

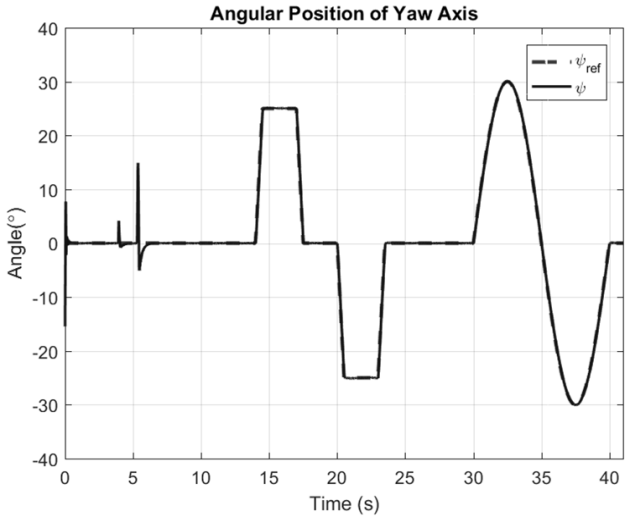

Fig. 7 Angular position of the yaw axis

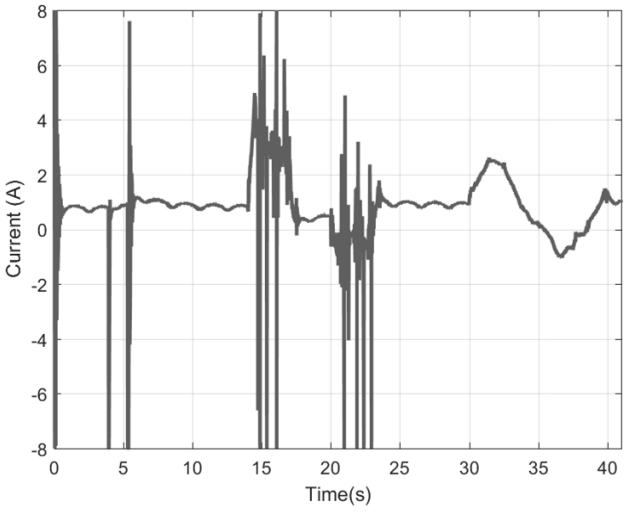

Fig. 8 Control input

In the figures above, angular position, velocity, current, and evolution of the sliding surface, and sliding sector are given respectively. In Fig. 6 the oscillation of the outer axis at constant frequency during the experiment is given. Throughout the experiment, the pitch axis is moved at a constant frequency and amplitude to create a gyroscopic effect on the yaw axis. Reference and actual angular position are given in Fig. 7. The system performs tracking of step and sinusoidal commands respectively. The disturbing effect is applied twice to the system around fifth seconds. As seen in the figure, the proposed controller successfully achieved robustness under different disturbances. In addition, the gimbal system successfully tracks both step inputs and sinusoidal input under the gyroscopic effect of the pitch axis by using the proposed SSC. In Fig. 8, the control effort of the system is shown. The control input is bounded by 8 Ampere by software to ensure the safety of the electromechanical system. Fig. 8 shows a high current requirement when disturbance inputs at around fifth seconds are active. In addition, when the steady-state error is zero in Fig.8, the need for sinusoidal current in Fig.9 draws attention due to the gyroscopic effect caused by the motion of the yaw axis. Finally, the state-dependent evolution of the sliding surface and sliding sector are presented. Due to the integral effect and the initial angle difference, in the case of zero command, the sliding surface value is different from zero and moves at the sector boundary. When the command is non-zero, the controller brings the system states into the sector and keeps them there. The states of the system move out of the sector when the disturbance effect is applied. Then the controller forces the state to the inside of the sector as seen in Fig. 9.

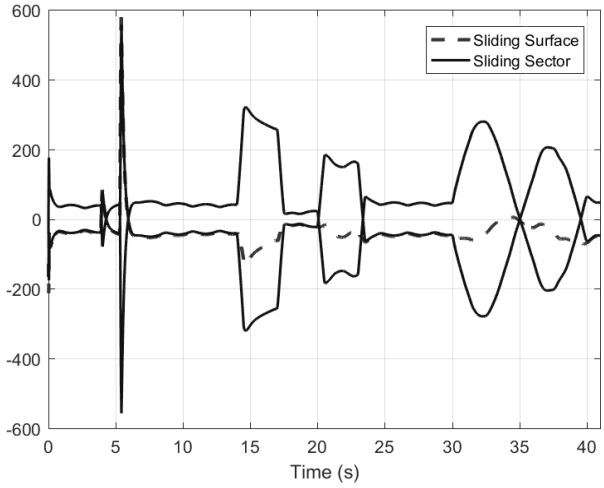

Fig. 9 Evolution of the sliding surface and sliding sectors

4. Conclusion

In this study, a new nonlinear state-dependent sliding sector control design methodology is proposed and it is then applied to a servo system. A two axes gimbal system is used for experimental testing of the proposed control method. It is shown that the proposed SSC method controls the nonlinear system successfully even when disturbances are exerted on the system. It is noted that the control parameters are not optimized in this study. The control structure and gains could be optimized and the torque caused by the gyroscopic effect could be reduced by considering further gain adjustments. Thus, the coupling

effect of the gimbal and similar mechanism could be minimized.

References

1. **Edwards, C.; Spurgeon, S.** 1998. Sliding Mode Control: Theory And Applications, Series in Systems and Control, Taylor & Francis. https://doi.org/10.1201/9781498701822.
2. **Utkin, V.** 2013. Sliding Modes in Control and Optimization, Communications and Control Engineering, Springer Berlin Heidelberg.
3. **Zhu, P.; Chen, Y.; Li, M.; Zhang, Wan Z.** 2020. Fractional-order sliding mode position tracking control for servo system with disturbance, ISA Transactions 105(2020): 269-277. https://doi.org/10.1016/j.isatra.2020.05.032.
4. **Han, X.; Fridman, E.; Spurgeon, S.** 2010. Sliding-mode control of uncertain systems in the presence of unmatched disturbances with applications, International Journal of Control 83(2010). https://doi.org/10.1080/00207179.2010.527375.
5. **Krupp, D.; Shtessel, Y. B.** 1999. Chattering-free sliding mode control with unmodeled dynamics, in: Proceedings of the American Control Conference 1: 530-534. https://doi.org/10.1109/ACC.1999.782884.
6. **Vo, A. T.; Kang, H.** 2019. A chattering-free, adaptive, robust tracking control scheme for nonlinear systems with uncertain dynamics, IEEE Access 7: 10457-10466.
7. **Alvarez-Rodriguez, S.; Flores, G.; Ochoa, N.** 2019. Variable gains sliding mode control, International Journal of Control, Automation and Systems. https://doi.org/10.1007/s12555-018-0095-9.
8. **Bartolini, G.; Pisano, A.; Punta, E.; Usai, E.** 2003. A survey of applications of second-order sliding mode control to mechanical systems, International Journal of Control 76: 875-892. https://doi.org/10.1080/ 00207017031000099010.
9. **Levant, A.** 2003. Higher-order sliding modes, differentiation and output-feedback control, International Journal of Control 76: 924-941. https://doi.org/10.1080/00207017031000099029.
10. **Furuta, K.; Pan, Y.** 2000. Variable structure control with sliding sector, Automatica 36: 211-228. https://doi.org/10.1016/S0005-1098(99)00116-8.
11. **Pan, Y.; Kumar, K.; Liu, G.; Furuta, K.** 2009. Design of variable structure control system with nonlinear time-varying sliding sector, Automatic Control, IEEE Transactions on 54: 1981-1986. https://doi.org/10.1109/TAC.2009.2023965.
12. **Xu, B.; Zhou, D.; Liang, Z.; Zhou, G.** 2016.Robust adaptive sliding sector control and control allocation of a missile with aerodynamic control surfaces and reaction jets, Proceedings of the Institution of Mechanical Engineers, Part G: Journal of Aerospace Engineering 231. https://doi.org/10.1177/0954410016638870.
13. **Özcan, S.; Salamci, M.; Nalbantoglu, V.** 2020. Nonlinear sliding sector design for multi-input systems with application to helicopter control, International Journal of Robust and Nonlinear Control 30. https://doi.org/10.1002/rnc.4877.
14. **Katebi, J.; Zamen, S.** 2016. Robust time varying sliding sector for uncertain structures control, Journal of Vibration and Control 24. https://doi.org/10.1177/1077546316636540.
15. **Hilkert, J. M.** 2008. Inertially stabilized platform technology concepts and principles, IEEE Control Systems Magazine 28 (1): 26-46. https://doi.org/10.1109/ 250 MCS.2007.910256.
16. **Masten, M. K.** 2008. Inertially stabilized platforms for optical imaging systems, IEEE Control Systems Magazine 28 (1): 47-64. https://doi.org/10.1109/MCS.2007.910201.
17. **Espinosa, C.; Mayen, K.; Lizarraga, M.; Romero, S.; Lozano, R.** 2015. Sliding mode line-of-sight stabilization of a two-axes gimbal system pp. 431-438. https://doi.org/10.1109/RED-UAS.2015.7441037.
18. **Naderolasli, A.; Tabatabaei, M.** 2016. Stabilization of the two-axis gimbal system based on an adaptive fractional-order sliding-mode controller, IETE Journal of Research 1-10. https://doi.org/10.1080/03772063.2016.1229581.
19. **Kurkcu, B.; Kasnakoglu, C. M.** 2018. Disturbance/uncertainty estimator based integral sliding mode control, IEEE Transactions on Automatic Control pp. 1-1. https://doi.org/10.1109/TAC.2018.2808440.
20. **Mao, J.; Li, S.; Li, Q.; Yang, J.** 2016. Continuous second-order sliding mode control based on disturbance observer for los stabilized system, pp. 394-399. https://doi.org/10.1109/VSS.2016.7506951.
21. **Xinli, Z.; Li, X.** 2019. A finite-time robust adaptive sliding mode control for electro-optical targeting system with friction compensation, IEEE Access 7: 166318-166328.
22. **Cimen, T.** 2008. State dependent riccati equation (sdre) control: A survey, Plenary Session of 17th IFAC World Congress 17. https://doi.org/10.3182/ 20080706-5-KR-1001.00635.
23. **Cimen, T.** 2010. Systematic and effective design of nonlinear feedback controllers via the state-dependent riccati equation (sdre) method, Annual Reviews in Control 34: 32-51. https://doi.org/10.1016/j.arcontrol.2010.03.001.
24. **Salamci, M.; Gokbilen, B.** 2007. Sdre missile autopilot design using sliding mode control with moving sliding surfaces, IFAC Proceedings Volumes (IFAC-PapersOnline) 17: 768-773.
25. **Suzuki, S.; Furuta, K.; Pan, Y.** 2003. State-dependent sliding-sector vs-control and application to swing-up control of pendulum, in: 42nd IEEE International Conference on Decision and Control (IEEE Cat. No.03CH37475), pp. 251-256. https://doi.org/10.1109/CDC.2003.1272569.
26. **Ozcan, S.; Salamci, M.; Birinci, B.** 2013. State dependent sliding sectors for nonlinear systems with nonlinear sliding surfaces pp. 5754-5759. https://doi.org/10.1109/ACC.2013.6580739.
27. **Copur, E. H.; Arican, A. C.; Ozcan, S.; Salamci, M. U.** 2019. An update algorithm design using moving region of attraction for sdre based control law, Journal of the Franklin Institute 356 (15): 8388 - 8413. https://doi.org/10.1016/j.jfranklin.2019.08.007.
28. **Slotine, J. J. E.; Li, W.** 1991. Applied nonlinear control.

29. **Bartolini, G.; Ferrara, A.; Usai, E.** 1997. Output tracking control of uncertain nonlinear second-order systems, Automatica 33 (12): 2203 - 2212. https://doi.org/10.1016/S0005-1098(97)00147-7.

B. E. Birinci, B. Özkan, M. U. Salamci

NONLINEAR STATE DEPENDENT SLIDING SECTOR CONTROL OF GIMBAL SYSTEMS

S u m m a r y

Sliding Sector Control (SSC) design method for nonlinear systems is proposed in such a way that the system trajectories are kept around a nonlinear sliding surface which is surrounded by a nonlinear sliding sector. The SSC for the nonlinear system is derived so that the system trajectories are enforced to stay inside the sliding sector for tracking requirements. State-Dependent Differential Riccati Equations (SDDRE) are solved to design the nonlinear sliding surface for the nonlinear dynamical system. Within this context, SSC having nonlinear(or state-dependent) sliding surfaces are used to have a viable solution for the problem formulation. The evolving solutions of the Differential Riccati Equations are used to create the sliding surface which is kept inside the designed sliding sector so that the stability of the nonlinear system is ensured. The proposed SSC method is experimentally tested by applying it to an inner axis of a two axes gimbal system.

Keywords: gimbal, nonlinear control systems, state dependent Riccati equations, sliding sector control.

Received April 25, 2022
Accepted October 17, 2022